PREPRINT UCRL- 79285

Conf-770434--7

Lawrence Livermore Laboratory

THE SHIVA LASER: NEARING COMPLETION

James A. Glaze and Robert O. Godwin

May 12, 1977

This Paper was Prepared for Submission to the
Society of Photo-Optical Instrumentation Engineers
SPIE Meeting, Reston, VA April 18-21, 1977

THE SHIVA LASER: NEARING COMPLETION*

James A. Glaze and Robert O. Godwin
Laser Fusion Program, Lawrence Livermore Laboratory
Livermore, California 94550

Abstract

Construction of the Shiva laser system is nearing completion. This laser will be operating in fall 1977 and will produce over 20 terawatts of focusable power in a subnanosecond pulse. Fusion experiments will begin early in 1978. It is anticipated that thermonuclear energy release equal to one percent that of the incident light energy will be achieved with sub-millimeter deuterium-tritium targets. From other experiments densities in excess of a thousand times that of liquid are also expected.

Introduction

The twenty-arm Nd:glass Shiva laser currently under development at the Lawrence Livermore Laboratory[1,2,3,4] is designed to explore advanced concepts in inertial confinement fusion. This laser is part of the 25M Congressionally funded High Energy Laser Facility at Livermore. This facility also includes a building which has been specifically designed to provide stringent environmental control of the laser and target chamber bays as well as space for energy storage, laser assembly and repair and support laboratories.

Figure 1 shows the project schedule. Major milestones for 1977 are operation and diagnostics of a single laser chain, and a full system demonstration of 10 kilojoules in a subnanosecond pulse.

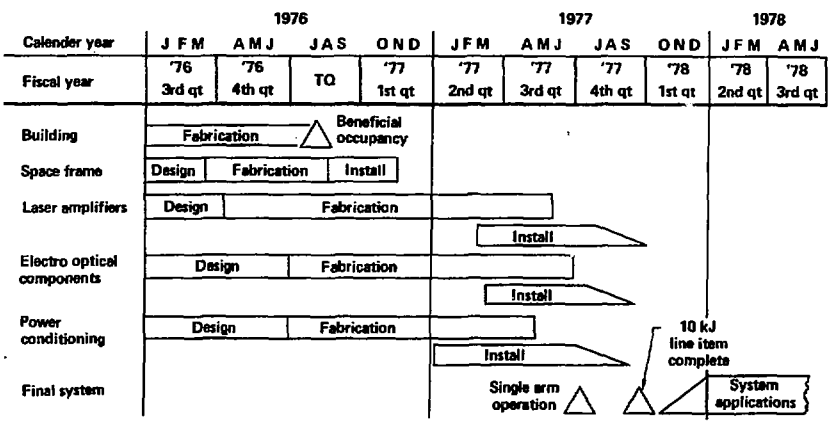

Fig. 1. High Energy Laser Facility Project Schedule.

System Design

Figure 2 shows a schematic of a single Shiva arm. Also shown is the calculated power performance at 0.1 and 1 nanoseconds, the capacitor bank energy delivered to the flashlamps in each amplifier module, the diameter of the clear aperture and the F-number of the beam relay and spatial filters. Small signal gains for the α and β rod amplifiers are 200 and 18 respectively while the gains of the β, γ and δ disk amplifiers are 3.7, 2.6 and 2 respectively.

*This work was performed under the auspices of the U.S. Energy Research and Development Administration. Contract Number W-7405-Eng-48.

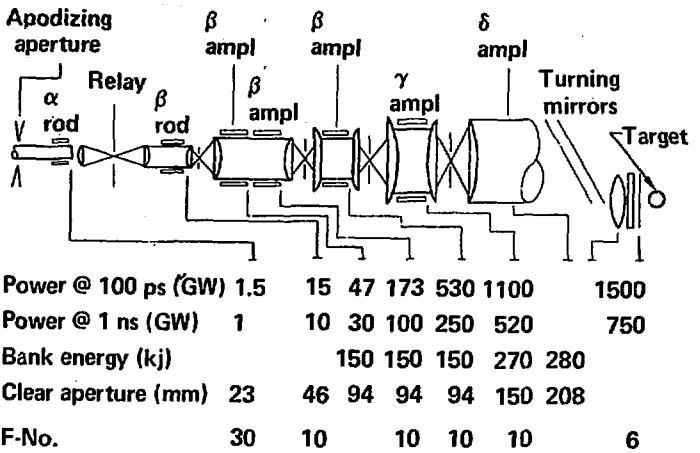

Fig. 2. Optical profile of a single Shiva laser chain. Representative values of laser power are given for 0.1 and 1 ns pulses at each stage. Also shown is the clear aperture of each amplifier and the electrical energy supplied to the flashlamps. All spatial filters are f/10 with the exception of the f/30 relay/filter located between the α and β rod amplifiers. Pinhole diameters for the filters range from 300 to 500 microns.

Figure 3 shows a plan schematic of the Shiva laser. The central portion of the figure shows the master oscillator and preamplifier sections along with a cw oscillator used for alignment and a cw mode-locked oscillator used to equalize the length of the optical paths to the target for the twenty chains. A pulse from a mode-locked YAG oscillator is first injected into a pulse shaper and then into preamplifier stages. The preamplifier stage consists of two α rod amplifiers, a β rod amplifier, a spatial filter and concomitant beam expansion telescopes, isolation stages and turning mirrors. A dye cell between the α and β rod amplifiers provides 20 dB of attenuation for both amplified spontaneous emission from the laser rods and prepulses from the oscillator. Following preamplification the pulse is divided into twenty channels and directed through the power amplifier chains to the target.

The major alignment systems are also indicated in Figure 3. The oscillator alignment system (OAS) was successfully prototyped at LLL and is now installed on the Shiva system. Pointing and centering accuracies are ± 2 microradians and ± 500 microns respectively at the input to the apodizing aperture. The chain input pointing system (CHIP) consists of an angle gimbal positioned in front of the apodizing aperture and a position sensor following this aperture. The gimbal has been purchased from Aerotech Corp., the sensor from Aerojet Electrosystems Co., and the controls designed and fabricated at LLL. This system has been fully prototyped and has achieved a pointing accuracy of ± 15 microradians. Pointing and focusing of the beams on target and centering of the beams on the final focusing lens is accomplished with two motorized gimbals, an imaging sensor and a three axis drive on the focusing lens. The sensor and final pointing gimbal have been designed by Aerojet Electrosystems Co. The first turning mirror gimbal and the lens drive system have been designed and built at LLL. The entire alignment system has been fully prototyped and evaluated on the Cyclops laser. Pointing, focusing and centering has been demonstrated to an accuracy of ± 1 μrad, ± 25 μm and ± 0.2 mm respectively. This performance meets or exceeds all projected Shiva requirements.

The optical components of the Shiva laser are mounted on two separate three-dimensional support structures constructed of square steel tubing[5]. Figure 4 shows a model of these structures as they appear in the laser and target bays of the High Energy Laser Facility. In the laser bay, the amplifier chains are mounted on the vertical faces of the two longitudinal columns. There are four and six amplifier chains respectively on the interior and exterior faces of each column. The components are mounted in cradles which are adjustable along the x and y axis. Each component can be rotated in its cradle for polarization setting. Arms that clamp the components in place can be swung out to allow crane access for fast and easy component replacement. Figures 5 and 6 show a β disk amplifier and spatial filter modules respectively mounted in cradles and attached to the support structure.

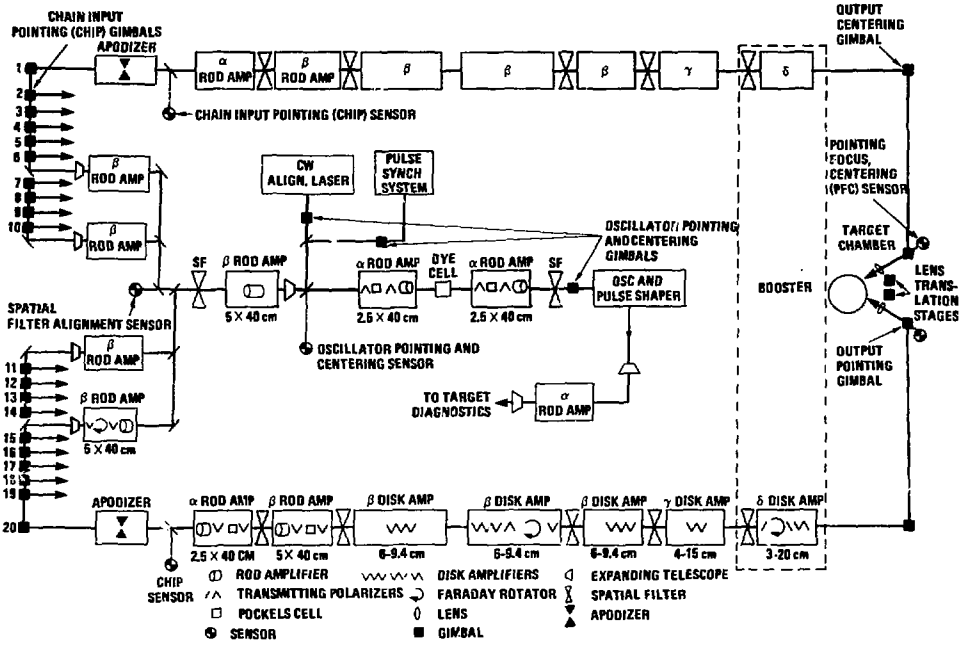

Fig. 3. Plan schematic of the Shiva laser system. The central portion of the figure shows pulse generation and preamplifier stages along with the oscillator alignment system and pulse synchronization system. The splitters and automated pointing gimbals to the left of the figure divide the beam into 20 amplifier channels. The output beam from each channel is directed to the target with an automated system of image sensors, pointing gimbals, and focusing lenses.

In the target bay the turning mirrors are supported on the faces of five towers which are interconnected in a pentagonal arrangement. These mirrors direct the laser beam into two opposing clusters of ten beams each. With this geometry, individual beams within a cluster are arranged on the corners of concentric pentagons with their polarization vector directed radially outward. Each beam is focused onto the target with f/6 singlet lenses attached to the target chamber. Figure 7 shows installation of the support towers in the target bay of the HELF.

Performance

Realistic performance models of the Shiva laser chain have evolved as a result of extensive experimentation with the Cyclops and Argus systems[6,7]. The Argus system in particular has provided a wealth of data on beam propagation, spatial filter transmission and power performance for pulses ranging from 30 ps to 1 ns. For the results of calculations presented below, both linear and nonlinear models of beam propagation, spatial filter transmission and gain saturation have been employed[8,9,10].

Figure 8 shows calculated performance curves for Shiva chains. From these curves it is observed that the output power is approximately constant for pulses shorter than 200 psec. In this range gain saturation is relatively unimportant and the power limited primarily by small scale self-focusing. For longer pulses the effects of saturation are clearly evident. Here the obtainable output power is limited by damage thresholds for optical coatings. In performing the calculations of Figure 8, the input power to the apodizing aperture for each pulse duration was constrained so that the peak flux at any chain location did not exceed 50% of

Beam Alignment

One of the new features being incorporated into the Shiva laser system is an electro-optical beam alignment system. Previous laser systems were manually aligned; however, because of the size and complexity of Shiva, an automatic alignment system is needed. The major elements of this alignment system are:

(1) oscillator pointing and centering;
(2) chain input pointing (CHIP);
(3) output pointing, focusing and centering (PFC);
(4) spatial filter alignment.

Since the mode-locked laser oscillator is not convenient for system alignment, a separate cw alignment laser is used. An oscillator pointing and centering system is used to establish and maintain collinearity of the mode-locked master oscillator and the cw alignment laser. These two laser beams have a relative angular accuracy of $\pm$ 2 microradians. The cw alignment laser is then used for the other alignment modes.

Following the beam splitter array, a chain input pointing (CHIP) sensor and gimbal steers the beam down each of the 20 chains.

At the output of the laser chain there are sensors and gimbals to point, focus, and center the beam. To sense the position of the beam center, a reflective screen placed in front of the focusing lens relays the beam to an optical imaging system. This system in turn images the plane of the lens (screen) onto a quadrant detector. Error signals from this detector are used to drive the output centering gimbals. The imaging system sensor is located behind the final turning mirror and along an axis passing through the center of the focusing lens and the center of the target chamber. Beam pointing is accomplished with the aid of a surrogate target placed at the center of the target chamber. The alignment beam, when incident on this sphere, is reflected backward through the focusing lens and into the imaging sensor. A quadrant detector provides error signals for the gimbal axis of the final turning mirror.

Following pointing and centering, focusing is accomplished by viewing the magnified image of the reflected beam on the TV screen. The size of this image is a measure of the distance from the surface of the surrogate target to the focus of the incoming beam. When this focus is midway between the target surface and its center, the smallest image diameter results. The operator simply adjusts the position of the focusing lens until the smallest image is obtained.

Spatial filter alignment is achieved by viewing the pinholes with vidicons while they are "back illuminated" by the alignment laser. One vidicon at the beam splitter array is used to align the two spatial filters prior to beam splitting. The vidicons in the incident beam diagnostics package are used to align the pinholes in each of the 20 arms.

In addition to the beam alignment systems, there is an optical path length sensor which allows the equalization of the path lengths for all 20 arms. This is an infrequent remote manual adjustment.

Figure 10 shows alignment system prototype hardware. The CHIP sensor is shown at upper left. These sensors are placed after the apodizing apertures in each chain. Angular error signals generated by a lateral photovoltaic detector are digitized and used to drive stepping motors on the CHIP angle gimbals shown below. These gimbals precede the apodizing aperture and are used to correct for pointing errors accrued in the beam splitter section.

The PFC sensor is shown at upper right. It is basically an f/2.5 imaging system with several angular magnification settings and contains a photovoltaic detector to provide error signals for the angle gimbals of the final turning mirror. A vidicon at the back of the sensor is used to view selected image planes for focusing adjustment and direct viewing of the target. An internal shutter protects the sensors from high power laser shots and also reflects the energy from such shots into a return beam diagnostics sensor attached to the side of the PFC package.

The output pointing mirror assembly is shown at lower left. Error signals from the PFC sensor drive stepping motors which are attached to torsion gimbals by heavy springs. This provides single step angular motions of 1 μrad with a total range of 5 mr. Rate damping of vibrational motions is provided by a tachometer attached to the torsion axis.

Figure 11 is a summary of the performance of the alignment system to date. Not shown is the performance of the Pulse Synchronization System used to equalize the optical path length to the target for each amplifier chain. This system employs a cw mode-locked oscillator and an optical heterodyne detector. It is currently under development at Hughes Aircraft Company of Culver City. In preliminary tests it has been used to detect path length changes of less than 1 mm with over 85 dB of attenuation in the signal arm.

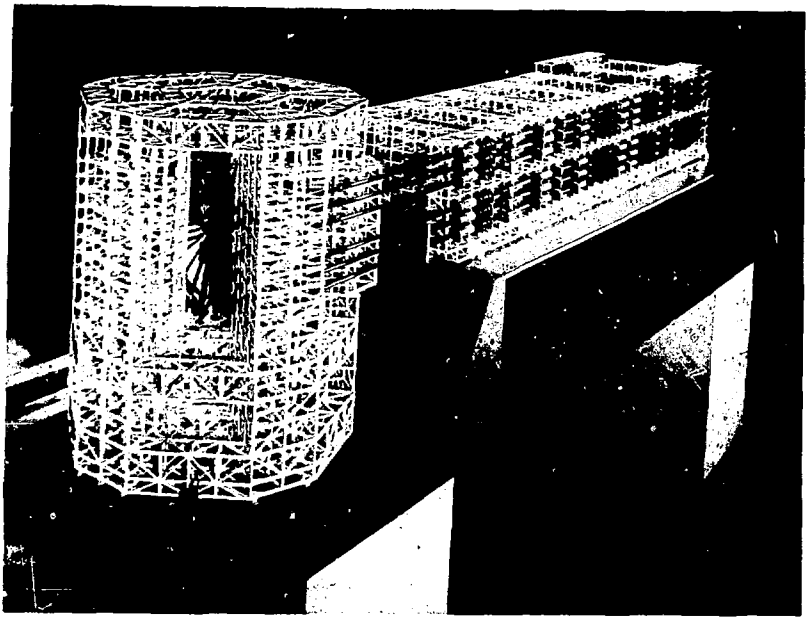

Fig. 4 Model showing laser and target chamber support structures as they appear in the high bay of the High Energy Laser Facility.

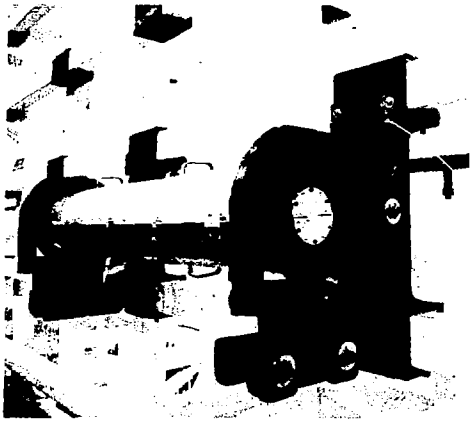

Fig. 5. Photograph of a β disk amplifier mounted to the laser support structure. The mounting cradles have adjustable x and y axis for ease in component alignment. Once mounted, the component can be rotated for polarization setting.

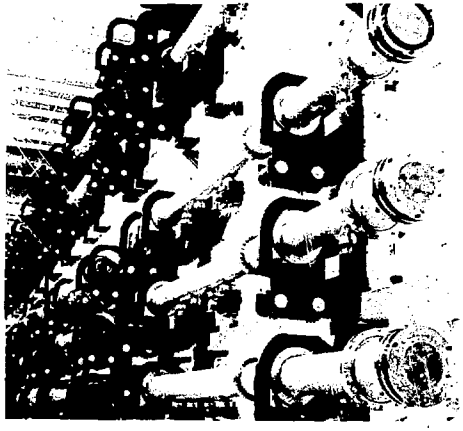

Fig. 6. Photograph showing spatial filters mounted in their support cradles, and attached to the laser support structure.

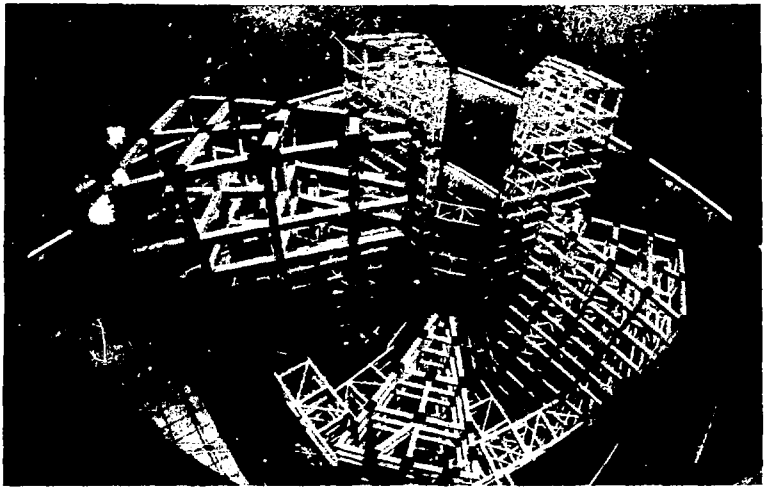

Fig. 7. Photograph of the target chamber support towers as they appeared during an early phase of installation.

the coating damage threshold. This limit, while somewhat arbitrary, has been imposed to insure safe operation even in the presence of moderate beam degradation caused by self-focusing and diffraction.

Figure 9 shows the expected far field intensity distribution from a ten beam cluster. The primary contribution to enlargement of the spot diameter is unfiltered small-scale self-focusing. Other contributors are diffraction, phase aberration, focal zoom, and pointing, focusing and lens positioning errors. The approximate brightness of the superimposed foci is estimated to be 10^{19} watts/cm^2-str.

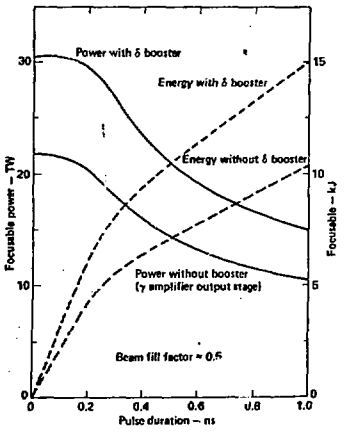

Fig. 8. Calculated focusable output power and energy from the Shiva amplifier chain for pulses up to 1 ns. The upper and lower curves correspond to chains with and without the 20 cm diameter δ amplifier booster stage.

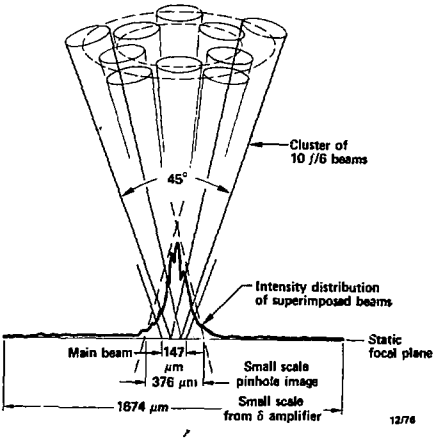

Fig. 9. Schematic of the calculated far field intensity distribution produced by a ten-beam cluster.

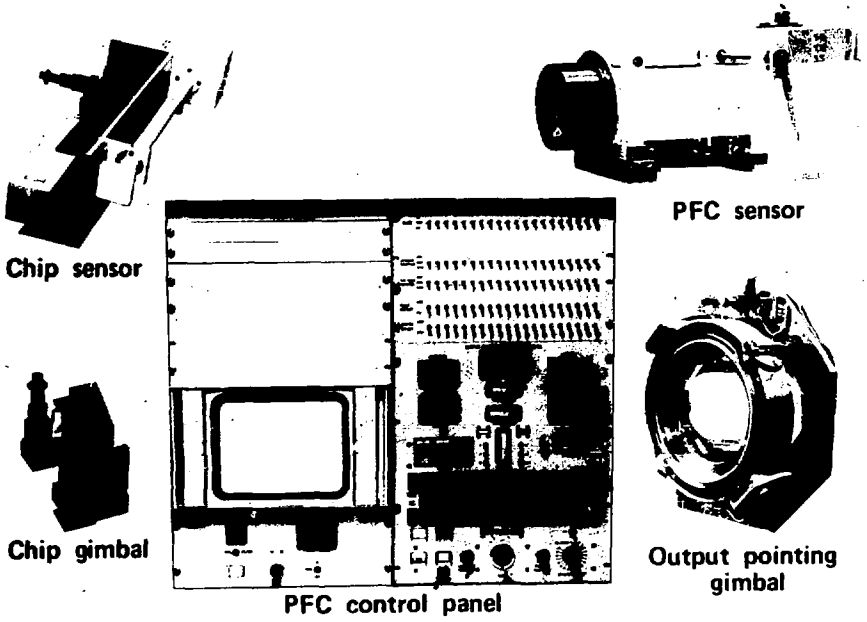

Fig. 10. Components of the automated alignment system.

Subsystem	Requirements		Performance (σ)	
	1975 estimate	Present estimate	Demonstrated to date	Expect to acheive
Oscillator coalignment Pointing	± 2 μr	± 20 μr	2.3 μr (CW) 3.5 μr (pulsed)	1 μr
Centering	± 1/2 mm	± 1/4 mm	1/10 to 1/4 mm	1/10 mm
Chain input pointing	± 60 μr	Same	± 15 μr	Same
Output pointing	± 1 μr	± 5 μr	± 1 μr	Same
Focusing	± 25 μm	± 60 μm	± 25 μm	Same
Centering	± 2 mm	Same	± 1/4 mm	Same

Fig. 11. Summary of requirements and performance of the automated alignment system.

Target Chamber

The target chamber with its concomitant diagnostics instrumentation is illustrated in Figure 12. The vacuum vessel is fabricated with 4.7 cm thick vacuum melted stainless steel. The focusing optics which are attached to the dome of the vessel are 220 mm diameter, F-6, BK7 lenses focusing through 15 mm thick vacuum windows and 3 mm debris shields. Diagnostics will measure neutron energy and spectrum, energy balance, alpha, beta, x-ray, optical and ion spectra, protons and time resolved x-ray emission of the imploding target. After the beams are pointed and focused with the use of a surrogate target, the foci are repositioned with 3-axis stepper motor lens positioners to within $\pm$ 5 μm of the desired point on the target. At the time of the shot the fusion pellet is substituted at the target point with a stepper motor driven 4-axis target positioner with $\pm$ 5 μm accuracy.

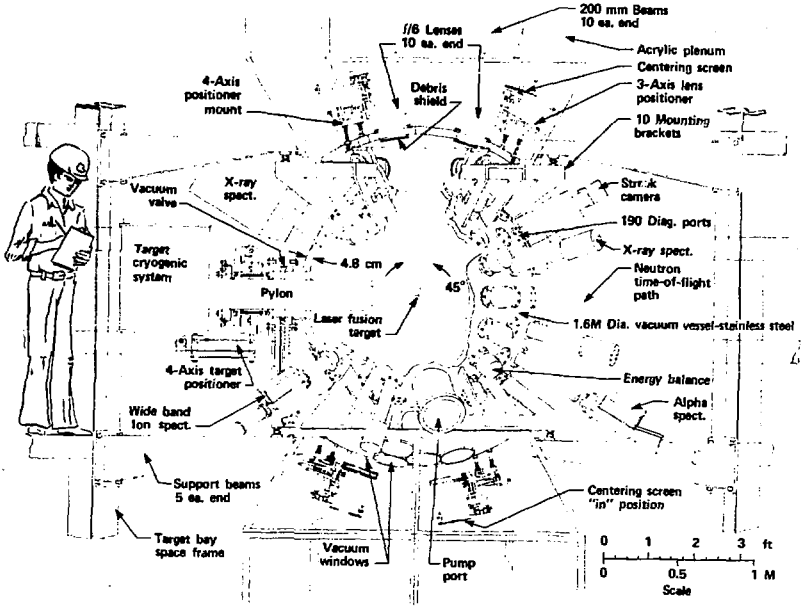

Fig. 12. Schematic of the Shiva target chamber with diagnostics instrumentation.

Laser Diagnostics

Extensive diagnostics are used to 1) optimize the performance of the laser system at all stages, 2) to provide laser data related to target performance and fusion diagnostics, and 3) isolate component failures.

Oscillator diagnostics includes measurement of prelase cavity power, sampling of the prelase pulse shape, recording of the output pulse shape, and recording and display of the switchout rejected pulse train. In addition the energy of the beam will be recorded at the output of the pulse shaper, and at the output of the α and β rod preamplifiers. The prelase level of the oscillator will be monitored with a slow photodiode coupled into a high gain amplifier, whose output is coupled to a microprocessor where it is digitized. The other pulse energy measurements are performed with pin photodiodes, whose outputs are first amplified by charge amplifiers and then digitized.

Chain diagnostics consist of measuring pulse energy with calibrated photodiodes at selected locations where high gain or potentially high loss mechanisms exist. To avoid inserting optical elements into the beam, energy will be collected from existing component reflections. Two sources of reflections at the desired monitoring points are available. These are reflections from the polarizers and reflections from the spatial filter lenses.

Oscillator prepulse energy and amplified spontaneous emission (ASE) can destroy the fusion target before the main pulse arrives. A combination of a dye cell and Pockels cells are used to suppress these sources. However both prepulse and ASE will be monitored for each shot on one of the Shiva amplifier chains.

The output of each beam will be monitored with a incident beam diagnostics sensor (IBD). This package, which is mounted in the target bay, will intercept 2-4% of the incident beam transmitted through the final turning mirror. The IBD will provide measurements of the total energy in each beam, the energy focusable to a given spot size in the equivalent target plane, far field multiple image arrays, and will contain a TV camera for pinhole alignment. Provisions are also made for attaching a streak camera to obtain the temporal shape of short pulses and a fast photodiode inside the IBD for long pulse temporal measurements.

There are also sensors attached to the PFC sensors to monitor light both reflected and refracted from the target.

Computer Control System

Because of its physical size and complexity, the Shiva laser system utilizes a greater amount of computer control than previous laser systems. However, to avoid having to develop one large central computer control system on the relatively short project schedule, the control system has been configured into four independent functional subsystems that can be designed, developed, and operated in parallel with a minimum of interaction. These four subsystems are shown in Figure 13.

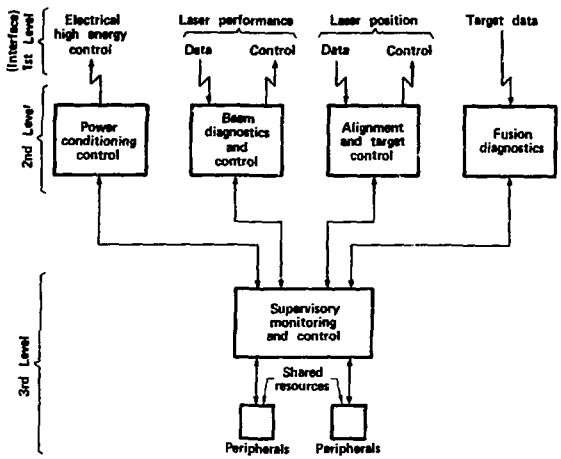

Fig. 13. Schematic of the Shiva computer control architecture.

The Power Conditioning Controls are responsible for the transformation storage and delivery the 25 megajoules of energy required for the Shiva laser. This subsystem controls the power conditioning from the 13.8 kV utility lines through to the flashlamps. In addition t as a failure diagnostics capability. This subsystem allows either direct manual intervention and control or automatic operation with manual supervision.

The Alignment and Target Positioning Control Subsystem controls all beam-handling equipment necessary for transporting the optical pulse from the oscillator through the 20 parallel laser paths onto the fusion target. This includes the control of mirror gimbals, lens motions, spatial filter pinhole positioners, and various shutters.

The Beam Quality Diagnostics and Control Subsystem is responsible for monitoring the laser performance with a combination of per-shot and periodic diagnostics. Typical per-shot diagnostics will include temporal pulse shape of the oscillator pulse, energy profile along each arm, energy output, energy reflected from the target, temporal pulse shape at the target, and prepulse energy at the target.

The Fusion Diagnostics Subsystem obtains experimental data from target shots. This subsystem is an upgrade of existing fusion data acquisition systems on the Argus and Janus laser facilities.

As shown in Figure 13, each of these subsystems have a 3 level hierarchical control network. At the first or lowest level are the Front End Processors (micro-computers) which perform the detail interface function both to the laser system components and the subsystem operators consoles. At the middle or "second level", each subsystem has its own independent control console and its own "Minicomputer". At the top or "3rd level" of the control system an overall facility control console integrates the operation of the four subsystems.

Projection

The Shiva system, when fully operational, will provide the experimenter with 20 to 30 terawatts of focusable power. With such power available, it should be possible to compress deuterium-tritium targets to densities a thousand times that of liquid. Also it is expected that significant thermonuclear burn yielding a few percent of light energy breakeven can be demonstrated. This will open the door to more ambitious programs in the early 80's designed to demonstrate laser fusion reactor feasibility. This of course will require larger lasers. System designs are currently underway that will permit the Shiva laser to be expanded to the 200 to 300 terawatt level. This will require larger aperture amplifiers and improved glass compositions. Both are well within the state-of-the-art today.

Acknowledgments

It is impossible to acknowledge adequately the many contributions that have led to the successes to date of the Shiva Project. The authors would like to thank the various Shiva Group Members through their group leaders, for their part in the formulation and execution of this difficult project. These leaders are C. Hurley, Mechanical Subsystems, W. Simmons, Laser Technology, W. Gagnon and P. Rupert, Power Conditioning, W. O'Neal, Target Chamber, R. Ozarski, Laser Diagnostics, F. Holloway, Electrooptical Controls, E. Bliss and M. Summers, Alignment System, P. Wallerstein, Optics, J. Trenholme and W. Hagen, System Analysis, and K. Manes, Laser Plasma Interaction. The authors would also like to thank J. Swain and R. Speck for their current efforts on system integration.

References

1. Laser Program Annual Report, (1975) UCRL 50021-75, (1976) UCRL 50021-76, Lawrence Livermore Laboratory.
2. T. J. Gilmartin, R. O. Godwin, J. W. Davis, W. F. Hagen, C. A. Hurley, G. W. Leppelmeier, G. J. Linford, J. J. Myall, W. C. O'Neal, and J. B. Trenholme, 10 Kilojoule Shiva Laser System for Fusion Experiments at LLL, 1975 IEEE/OSA Conference on Laser Engineering and Applications, May 28-30, 1975.
3. J. A. Glaze, W. W. Simmons and W. F. Hagen, Status of Large Neodymium Glass Lasers, SPIE Proceedings, Vol. 76, p. 7, 1976.
4. R. O. Godwin, Shiva Laser System for Fusion Experiments, 1976 Meeting of the Electro-optical Systems Design Conference/International Laser Exposition (Electro-optics '76), Sept. 14-16, 1976, New York.
5. C. A. Hurley and J. O. Myall, High Stability Spaceframe for a Large Fusion Laser, Sixth Symposium on Engineering Problems of Fusion Research, Nov. 17-21, 1975.
6. J. A. Glaze, High Energy Glass Lasers, Optical Engineering, Vol. 15, No. 2, March-April 1976.
7. W. W. Simmons, In Pursuit of Fusion; Argus Laser System at Livermore, European Conference on Laser Interaction with Matter, Palaiseau France, October 18-22, 1976.
8. J. B. Trenholme, Lumped-Element Analysis of Laser Systems, UCRL 50021-76, Lawrence Livermore Laboratory Laser Program Annual Report - 1976.
9. W. F. Hagen, Laser System Design and Analysis, UCRL 50021-76, Lawrence Livermore Laboratory Laser Program Annual Report - 1975.
10. J. T. Hunt, P. A. Renard and R. G. Nelson, Focusing Properties of an Aberrated Laser Beam, Appl. Opt. 15, 1458 (1975).
11. W. C. O'Neal, J. A. Monjes, and F. Rienecker, Jr., Many-Beam Target Chamber for Laser Fusion Experiments, UCRL-78991, Lawrence Livermore Laboratory.